Published in final edited form as:
Mol Cancer Res. 2015 February ; 13(2): 380–390. doi:10.1158/1541-7786.MCR-14-0303.

The chemokine (CCL2-CCR2) signaling axis mediates perineural invasion

Shizhi He[1,2], **Shuangba He**[1,3], **Chun-Hao Chen**[1], **Sylvie Deborde**[1], **Richard L. Bakst**[4], **Natalya Chernichenko**[1], **William F. McNamara**[1], **Sei Young Lee**[1], **Fernando Barajas**[1], **Zhenkun Yu**[5], **Hikmat A. Al-Ahmadie**[6], and **Richard J. Wong**[1]

[1]Department of Surgery, Memorial Sloan-Kettering Cancer Center, New York, NY, 10021

[2]Department of Otolaryngology-Head and Neck Surgery, Beijing Tongren Hospital, Capital Medical University, Beijing, P.R. of China, 100730

[3]Department of Otolaryngology-Head and Neck Surgery, Anhui Provincial Hospital, Anhui Medical University, Anhui, China, 230001

[4]Department of Radiation Oncology, Mount Sinai Hospital, New York, NY, 10029

[5]Department of Otolaryngology-Head and Neck Surgery, Nanjing Tongren Hospital, Nanjing, P.R. of China, 211102

[6]Department of Pathology, Memorial Sloan-Kettering Cancer Center, New York, NY, 10021

Abstract

Perineural invasion (PNI) is a form of cancer progression where cancer cells invade along nerves. This behavior is associated with poor clinical outcomes; therefore, it is critical to identify novel ligand-receptor interactions between nerves and cancer cells that support the process of PNI. A proteomic profiler chemokine array was used to screen for nerve-derived factors secreted from tissue explants of dorsal root ganglion (DRG), and CCL2 was identified as a lead candidate. Prostate cancer cell line expression of CCR2, the receptor to CCL2, correlated closely with MAPK and Akt pathway activity and cell migration towards CCL2 and DRG. In vitro nerve and cancer co-culture invasion assays of PNI demonstrated that cancer cell CCR2 expression facilitates PNI. PNI is significantly diminished in co-culture assays when using DRG harvested from CCL2−/− knockout mice as compared with control CCL2+/+ mice, indicating that CCR2 is

Corresponding Author: Richard J. Wong, MD, Department of Surgery, Memorial Sloan-Kettering Cancer Center, 1275 York Avenue, C-1069, New York, NY 10021, Phone: 212-639-7638, wongr@mskcc.org, Fax: 212-717-3302.

Conflicts of Interest
The authors declare no conflicts of interest.

Author Contributions
Shizhi He – design, execution and interpretation of data, article preparation
Shuangba He – design, execution and interpretation of data
CHC – design, execution and interpretation of data, article preparation
SD – execution and interpretation of data
RLB – conception, interpretation of data
NC, WFM, SYL, ZY – interpretation of data
FB – execution of data
HAA – execution and interpretation of data
RJW – conception, design, interpretation of data, article preparation

required for PNI in this murine model of PNI. Furthermore, 20/21 (95%) of patient specimens of prostate adenocarcinoma with PNI exhibited CCR2 expression by immunohistochemistry, while just 3/13 (23%) lacking PNI expressed CCR2. In summary, nerve-released CCL2 supports prostate cancer migration and PNI though CCR2-mediated signaling.

Keywords

paracrine; migration; microenvironment

Introduction

Prostate cancer currently is the most common cancer and the second leading cause of cancer death in American men (1). Mortality in prostate cancer patients is generally attributable to extracapsular spread, which often results in treatment failure and is associated with poor prognosis (2). Perineural invasion (PNI) is defined as the invasion of cancer cells in, around, and through nerves (3). Multiple studies have shown an association between the presence of PNI in prostate cancer and both higher pathological stage and Gleason score (4). PNI is highly prevalent in prostate cancer, observed in as many as 80% of resected prostate cancer specimens and in 20% of biopsies from patients without lymph node metastases (5–7). Current theories suggest that PNI is a key route of extracapsular spread in prostate cancer (8).

The molecular mechanisms underlying PNI remain poorly understood. Recent theories have suggested that nerve microenvironment may release chemotactic factors that attract cancer cells to migrate towards nerves (9–11). Our group recently demonstrated that glial-derived growth factor (GDNF), secreted by nerves, induces pancreatic cancer cell migration and PNI through RET receptor phosphorylation and downstream MAPK signaling (12). These findings implicate GDNF-RET signaling as playing a central role in the process of pancreatic cancer PNI. However, in these studies, the inhibition of GDNF secretion by nerves only partially blocks cancer cell perineural invasion, suggesting that other unidentified ligand-receptor interactions are also playing a role. Furthermore, when radiation is used to disrupt nerves and nerve supporting cells, PNI can only be partially reconstituted by the addition of exogenous GDNF (13). These results suggest that other nerve-secreted factors likely play a contributing role in the process of PNI. Other studies have also suggested that a variety of other ligand-receptor interactions play a role in PNI (3, 9).

Chemokines are a family of small soluble proteins that regulate cell migration through the formation of concentration gradients (14). These proteins exhibit a high degree of conservation between mice and humans and are critical mediators of immune cell trafficking during embryonic development, wound healing, and infection (15). Interestingly, chemokines and their receptors have been implicated in tumor growth and invasion (16–18). Chemokines may elicit cancer cell mobilization and promote distant metastasis with organ selectivity (19–21). The chemokine receptor CXCR4 is increased in metastatic prostate cancer as compared with localized prostate cancer (22), and CXCR1 is correlated with more aggressive prostate cancer of higher Gleason score and lymph node metastases (23). CCL2-

CCR2 signaling may also stimulate prostate cancer cell migration through a layer of bone marrow endothelial cells (24).

In this study, we used a chemokine profiling array to screen factors produced by dorsal root ganglion (DRG) that may potentially mediate PNI. We use DRG as part of an *in vitro* co-culture assay with cancer cells as a model of PNI. The screen identified CCL2 as a chemokine that is expressed by DRG. Interestingly, CCL2 has been shown to be a critical modulator of inflammation, regulating monocyte recruitment during wound healing, infections, and autoimmune diseases. CCR2, the receptor to CCL2, may be expressed in prostate and other cancer cell lines. These results prompted us to evaluate the role of the CCL2-CCR2 signaling in prostate cancer cells during the process of PNI.

Materials and Methods

Cell lines and mice

A panel of human carcinoma cell lines were purchased from the American Type Culture Collection (Manassas, VA), including prostate carcinoma (PC-3, DU145, LNCap), pancreatic adenocarcinoma (MiaPaCa2, Panc1), head and neck squamous cell carcinoma (SCC25), and thyroid medullary carcinoma (TT) cell lines. A lung mucoepidermoid carcinoma cell line (H292) was a gift from Dr Frederic Kaye (National Cancer Institute). PC-3, DU145, MiaPaCa2, Panc1, SCC25 and H292 were grown in vitro in Dulbecco's modified Eagle medium (DMEM). LNCap was grown in RPMI-1640, and TT was grown in F-12K. Cells were grown in 10% fetal calf serum with penicillin and streptomycin, and incubated in 5% CO2 at 37°C.

All mouse studies were performed in accordance with institutional protocol guidelines at Memorial Sloan-Kettering Cancer Center (MSKCC). Mice were maintained according to NIH Animal Care guidelines, under protocols approved by the MSKCC Institutional Animal Care Committee. Athymic nude mice were purchased from Harlan Laboratory (Indianapolis, IN), and Balb/c mice from Charles River Laboratory (Wilmington, MA). C57BL/6J mice were purchased from The Jackson Laboratory (Bar Harbor, ME). C57BL/6J CCL2−/− mice were obtained from Dr. Eric G. Pamer (Memorial Sloan-Kettering Cancer Center, New York, NY) (25). DRG were isolated from mice as previously described (26).

Reagents

Recombinant human CCL2 was purchased from R&D Systems (Minneapolis, MN). A rabbit polyclonal anti-CCL2 antibody for Western blotting was purchased (ab7202, Abcam, Cambridge, MA). A monoclonal anti-CCL2 antibody was obtained for neutralization of CCL2 (MAB479, R&D Systems, Minneapolis, MN). A rabbit polyclonal anti-CCR2 antibody for Western blotting was purchased (ab21667, Abcam). A rabbit monoclonal anti-CCR2 antibody was obtained for immunohistochemistry (E68, Novus Biologicals, Littleton, CO). Anti-GAPDH (glyceraldehyde-3-phosphate dehydrogenase) antibody was purchased from EMD Millipore (Billerica, MA). Anti-pMEK1/2, anti-MEK1/2, anti-pAkt, and anti-Akt antibodies were obtained from Cell Signaling Technology (Beverly, MA). Alexa Fluor® 568 Goat Anti-Rabbit IgG (H+L) was purchased from Life Technologies (Grand

Island, NY). Growth factor-depleted Matrigel matrix was purchased from BD Biosciences (Bedford, MA).

Chemokine array

Chemokines secreted by dorsal root ganglia (DRG) were screened using a Proteome Profiler Mouse Chemokine Array Kit (R&D Systems; Minneapolis, MN) according to the manufacturer's instructions. The array consists of 25 different mouse chemokines spotted in duplicate onto four membranes. Conditioned media using DMEM without FCS was collected after 24 hours of exposure to 7 day old murine DRG explants. Array membranes were incubated for 1 h in blocking buffer and then incubated overnight with 1 mL of conditioned media or DMEM with no FCS as control, and then combined with the detection antibody cocktail. The membranes were washed and incubated with streptavidin-horse radish peroxidase (HRP) and Chemi Reagent Mix.

Boyden chamber migration assays

Polyethylene terephthalate inserts with 8.0 μm pores (BD Biosciences, Bedford, MA) were used in 24-well plates for migration assays. Cells were grown in 0.1% FCS media overnight, and 5×10^4 cells were added in 0.5 mL of media into each insert. Media (0.7 mL) with 0.1% FCS was added to each of the lower wells using CCL2 (0, 10, or 25 ng/mL) or DRG explants as attractants. In additional experiments, DRG were treated with anti-CCL2 antibody (1 or 10 μg/mL), or with 10 μg/mL isotype IgG as a control. The inserts were removed after 18 hours. Non-migrating cells were wiped off from the superior aspect of the membranes with a cotton swab. Migrating cells on the undersurface of the membrane were fixed in 100% alcohol for 10 minutes and stained with 1% methylene blue in 1% borax for 20 minutes. Membranes were excised and mounted on glass slides. Cells were counted at five high-power fields (X200) at predetermined areas of the membrane.

Western blotting

Cells or DRG from CCL2 −/− and CCL2 +/+ mice were placed in serum-free media for one day. Cells were treated with CCL2 (25 ng/ml) for varying periods. Cell lysates were prepared using IP lysis buffer (Thermo Fisher Scientific, Rockford, IL). DRG were lysed using N-PER neuronal protein extraction reagent (Thermo Fisher Scientific, Rockford, IL). Conditioned media was collected from the DRG culture with or without anti-CCL2 antibody (1 or 10 μg/mL) after 15 minutes. All samples were measured for total protein content using a Bradford assay (Bio-Rad, Hercules, CA) to insure equal loading. Protein was subjected to electrophoresis in 7.5% Tris-HCl gels (Bio-Rad, Hercules, CA) and transferred to polyvinylidene difluoride membranes. The membranes were blocked with 5% nonfat dry milk in 0.1% Tween in Tris-buffered saline (Bio-Rad, Hercules, CA), and incubated with primary antibody (CCR2 antibody at 1μg/ml) overnight followed by a secondary antibody conjugated to horseradish peroxidase. Protein-antibody complexes were exposed to light-sensitive film using an ECL Plus Detection System (GE Healthcare Bio-Sciences, Pittsburgh, PA). GAPDH (glyceraldehyde-3-phosphate dehydrogenase) was used as a loading control.

Lentiviral shRNA transfection

MISSION® shRNA bacterial glycerol stocks containing four different constructs targeting CCR2 were purchased from Sigma-Aldrich (St. Louis, MO). Plasmids were packaged with MISSION® Lentiviral Packaging Mix (St. Louis, MO) and transfected using Lipofectamine 2000 transfection reagent (Life Technologies, Grand Island, NY) into HEK293T cells (ATCC, Manassas, VA). After transfection, media was changed and lentivirus was collected 48 hours later and filtered through 0.45 μm filters. Cells were infected with lentivirus in the presence of polybrene (8μg/ml). Forty eight hours later, cells were treated with 1 mg/mL of puromycin to select resistant clones. MISSION® shRNA Control Transduction Particles (SHC001V) were used as a control. The following shRNA targeting CCR2 were tested: sh1676 5′-CCG GCC CAG GAA TCA TCT TTA CTA ACT CGA GTT AGT AAA GAT GAT TCC TGG GTT TTT-3′; sh1677 5′-CCG GGC TGC AAA TGA GTG GGT CTT TCT CGA GAA AGA CCC ACT CAT TTG CAG CTT TTT-3′; sh1678: 5′-CCG GCC TCA TCT TAA TAA ACT GCA ACT CGA GTT GCA GTT TAT TAA GAT GAG GTT TTT-3′; sh1679 5′-CCG GGC CAG AAA GAA GAT TCT GTT TCT CGA GAA ACA GAA TCT TCT TTC TGG CTT TTT-3′.

In vitro DRG co-culture model of perineural invasion

The *in vitro* DRG co-culture model of perineural invasion is based on a technique originally described by Ayala (27), and refined by our group (12–13). Excised murine DRG are implanted in the center of a 10 μl drop of growth factor reduced Matrigel (BD Biosciences Bedford, MA). PC-3, shControl PC-3, and shCCR2 PC-3 cells were labeled with 25 μM of the fluorescent CellTracker Green CMFDA (5-chloromethylfluorescein diacetate; Molecular Probes, Invitrogen, Carlsbad, CA) for 1 h at 37°C. At day 7 after DRG implantation, 2×10^4 cancer cells were seeded in the DRG media. Two, three and four days after the cancer cells were added, plates were scanned on an Axiovert 200M microscope (Carl Zeiss, Oberkochen, Germany) and images acquired using a Photometrics Coolsnap ES camera (Photometrics, Tucson, AZ). Areas of nerve invasion, defined as fluorescent cancer cells in association with DRG neurites, were outlined and quantified by MetaMorph software (MetaMorph 7.7.4; Molecular Devices, Sunnyvale, CA).

In vivo model of sciatic nerve invasion

Nude athymic mice were anesthetized with isoflurane (5% for induction, 2% for maintenance; Baxter Healthcare Corp., Deerfield, IL) and their right sciatic nerves were surgically exposed. Ten mice were distributed randomly into two groups. shControl PC-3 cells (2×10^5) and shCCR2 PC-3 cells (6×10^5) in 3 μl volume of PBS were microscopically injected into the distal sciatic nerve, under the epineurium, using a 10-μl Hamilton syringe as previously described (12, 13). Additional mice underwent sciatic nerve injection with PBS as non-tumor bearing controls. The sciatic nerve innervates the hind limb paw muscles. Sciatic nerve function was measured weekly as described previously (12, 28) using the following the (a) *sciatic neurological score*, which grades hind limb paw response to manual extension of the body, from 4 (normal) to 1 (total paw paralysis); and (b) *sciatic nerve function index*, which measures the spread width between the first and fifth toes of the hind

limbs. These measures were normal in all mice immediately after surgical implantation of the cancer cells.

MRI assessment of in vivo perineural invasion

Murine sciatic nerve tumors generated from shControl PC-3 cells and shCCR2 PC-3 cells were assessed by magnetic resonance imaging (MRI). A Bruker USR 4.7T 40 cm bore scanner (Bruker Biospin MRI GmbH, Ettlingen, Germany) equipped with a 400 mT/m 12-cm bore gradient, using a custom-designed active decoupled radiofrequency surface coil (Stark MRI Contrast Research, Erlangen, Germany). After the mice were anesthetized with isoflurane, sciatic nerves were localized by a scout fast spin echo scan in three orientations, followed by a coronal T2-weighted fast spin-echo image acquired with: TR/TE 1.9 s and 40 ms, 117 × 186 μm in-plane resolution, 16 slices of 0.8 mm slice thickness and 12 averages. Images were used to visually assess the caliber of the sciatic nerve as it courses proximal to the primary tumor injection site. Sciatic nerve invasion length based on MRI imaging was assessed. Images showing a thickened sciatic nerve were analyzed with ImageJ.

Histology of perineural invasion by prostate cancer in vivo

Sciatic nerve and tumor specimens were excised from mice, frozen in OCT (Sakura Finetek, Torrance, CA), and cut into 8 μm thick sections on glass slides. Slides were fixed and stained with hematoxylin and eosin. To assess CCR2 expression, immunofluorescence staining of adjacent cuts was performed at a dilution of 1:100. Slides were fixed with 2% formaldehyde and 0.2% glutaraldehyde, quenched, blocked, and incubated with primary antibodies overnight at 4°C. Slides were incubated with Alexa Fluor® 568 Goat Anti-Rabbit IgG at a 1:500 dilution for 1 hour at room temperature, washed again, and treated with 5μg/ml DAPI (4′, 6-diamidino-2-phenylindole) solution for 5 minutes at room temperature. Images were captured on a Zeiss microscope (Zeiss LSM510 Inverted Confocal, AxioVert 200M; Hamburg, Germany) and acquired by Mirax slide scanner (20 x/0.8 NA objective) using Mirax scan software (Carl Zeiss, Oberkochen, Germany).

Five human prostate cancer specimens exhibiting perineural invasion were formalin-fixed and paraffin embedded and cut into 4 micron thick sections. A Ventana XT (Tucson, AZ) platform was used for immunohistochemistry, using a primary anti-CCR2 antibody (E68, Novus Biologicals, Littleton, CO) at 1:400 dilution, and a one hour incubation period. Detection was performed with the DAB Map Ventana detection system (Tucson, AZ).

Statistical analysis

A student t-test was used for statistical analysis as appropriate. All P values were calculated using two-sided tests. Statistical significance was determined as $p < 0.05$. Error bars in the graphs represent standard error of the mean.

Results

Dorsal root ganglia express CCL2

To identify chemokines produced by dorsal root ganglia, which support cancer PNI in our *in vitro* co-culture assays, we used a chemokine array kit to screen conditioned media from

DRG cultures. Of 25 chemokines included in the array, we identified the overexpression of six: CCL12, CCL6, chemerin, IL-16, CXCL1, and CCL2 (Fig. 1A). Densitometry analysis of the chemokine array signal was performed using ImageJ (rsbweb.nih.gov/ij) and normalized to the average intensity of the 3 controls (Sup Fig. 1). CCL12 and CCL6 were excluded, as they have been identified only in rodents. Of the remaining candidates, chemerin is an adipokine that regulates adipogenesis and adipocyte metabolism, while IL-16 is a T lymphocyte attractant. CXCL1 is a chemokine that recruits neutrophils and has been implicated in melanoma pathogenesis. CCL2 is a chemokine involved in macrophage recruitment, inflammation, and may also induce prostate cancer migration. CCL2 was selected for further evaluation. CCL2 expression by DRG was validated by Western blot (Fig. 4A).

Expression of CCR2 by cancer cell lines correlates with CCL2-induced cell migration

CCL2 exhibits strong binding affinity to the chemokine receptor CCR2, and signals primarily through CCR2 in monocytes and macrophages to regulate migration. We assessed CCR2 expression in the cancer cell lines PC-3, DU145, LNCap, MiaPaCa2, Panc1, and SCC25. Using western blot analysis, CCR2 expression was detected in 4 of 6 lines tested (Fig. 1B). We next assessed whether recombinant CCL2 protein could induce cancer cell migration in these cell lines using Boyden chamber migration assays. CCR2 positive cancer cells PC-3, DU 145, and H292 show increases in migration in response to CCL2 in a dose-dependent manner up to 25ng/ml (Fig. 1C). Panc1 expresses a lower level of CCR2, and responded to CCL2 only up to 10ng/ml. In contrast, MiaPaCa2 and LNCap demonstrate low expression of CCR2 and were unresponsive to CCL2.

CCR2 expression by PC-3 is required for CCL2-dependent migration

We next used an shRNA approach to silence CCR2 expression in PC-3 cells. Western blot confirmed successful depletion of CCR2 protein by shRNA1678, as compared to three other hairpins targeting CCR2 and shControl (Fig. 2A). Therefore, shRNA1678 was selected to silence CCR2 in PC-3. There were no significant differences in cell proliferation between shControl PC-3 and shCCR2 PC-3 over four days, although by later days the shControl cells exhibited a more rapid growth (Fig. 2B). As migration assays were concluded by 18 hours, these findings eliminate a proliferation deficit of shCCR2 cells as a confounder in these studies. In migration assays, shControl PC-3 cells remain responsive to CCL2 in a dose dependant manner (Fig. 2C). In contrast, shCCR2 PC-3 cells demonstrated a lack of migration in response to CCL2 stimulation (Fig. 2D).

When live explants of DRG in Matrigel are used to attract PC-3 (Fig. 2E), far more robust migration is demonstrated than with CCL2 alone (Fig. 2C). We tested whether antibody inhibition of CCL2 secreted from the DRG could inhibit prostate cancer cells migration. Adding anti-CCL2 neutralizing antibody at 10 μg/ml to the DRG in the lower chamber reduced PC-3 migration by 33% (Fig. 2E), suggesting a significant role of CCL2 signaling in mediating prostate cancer cell migration towards nerves. The addition non-specific rat IgG at 10 μg/ml showed no inhibitory effects, in contrast to the anti-CCL2 antibody (Sup. Fig. 2). The partial inhibition with the anti-CCL2 antibody suggests either incomplete CCL2 inhibition by this antibody, or the presence of factors other than CCL2 secreted by the DRG

that may support PC-3 migration. We next used DRG as an attractant for shControl and shCCR2 PC-3 cells. The loss of CCR2 expression reduced PC-3 cell migration towards nerves by 43% (Fig. 2F), which is slightly more pronounced than the migration reduction noted by the blocking anti-CCL-2 antibodies (Fig. 2E). These findings suggest that CCL2 plays a significant, though partial, role in inducing PC-3 cell migration towards DRG.

CCL2 activates the MAPK and Akt pathways in prostate cancer

We sought to identify potential signaling pathways involved in CCL2-induced cell migration. CCL2 phosphorylates Akt in PC-3 cells in protecting cells against autophagy (29). We demonstrate that p-MEK1/2 and p-Akt expression are both increased in PC-3 cells by 15 minutes after exposure to CCL2 at 25 ng/ml (Fig. 2G). To validate this effect using DRG, PC-3 cells were exposed to conditioned media collected from DRG, with or without anti-CCL2 antibody, and then underwent protein isolation. Both p-MEK1/2 and p-Akt were activated by DRG conditioned media. However, with the addition of anti-CCL2 antibody at 10μg/mL, p-Akt expression was nearly completely inhibited, while p-MEK1/2 expression was partially reduced (Fig. 2H). These data demonstrate that CCL2 induces Akt and MAPK pathway activation in PC-3 cells.

CCR2 expression by prostate cancer facilitates perineural invasion in vitro

We assessed whether CCR2 is required for prostate cancer perineural invasion using a DRG co-culture *in vitro* model to quantify cancer-nerve interactions. In this model, surgically excised murine DRG are grown in a drop of growth factor depleted Matrigel, and fluorescent cancer cells are subsequently added to the media. Cancer cells may then invade into the Matrigel, attach to the DRG neurites (axonal-like projections) and migrate towards the center of the DRG along these neurites (12–13) in a model of perineural invasion (Sup. Fig. 3A). The fluorescent cancer cells which extend along neurites may be outlined, and the area measured with MetaMorph software (Fig. 3C–E).

We found a significant reduction of the area of perineural invasion by the shCCR2 PC-3 cells as compared with shControl PC-3 cells (Fig. 3A–B, 3F, $p<0.05$, t-test). To exclude the possibility of cancer cells randomly adhering to or invading the Matrigel, we seeded shControl and shCCR2 PC-3 cells on Matrigel without any DRG, as a negative control (Fig. 3A–B).

CCL2 release by DRG facilitates prostate cancer perineural invasion in vitro

To confirm that CCL2 released from DRG is inducing migration and PNI, we obtained CCL2−/− homozygous deleted mice. Western blot confirmed lower CCL2 expression by the DRG of CCL2−/− mice as compared with the DRG from wild type CCL2+/+ mice (Fig. 4A). Cultured DRG from both wild type and CCL2−/− mice generate equitable neurite areas (Sup. Fig. 4B), although the CCL2−/− DRG occasionally fail to grow in culture. Boyden chamber assays were performed with PC-3 cells using CCL2−/− DRG or CCL2 +/+ DRG as a chemoattractant. Quantification demonstrated a 35% reduction of migrating PC-3 towards CCL2 −/− DRG as compared to CCL2+/+ DRG (Fig. 4B, $p<0.05$, t-test). We then performed DRG co-culture assays to assess for PNI *in vitro.* DRG harvested from CCL2+/+ and CCL2−/− mice exhibited similar morphology and neurite growth patterns. However, the

area of nerve invasion by the PC-3 cells was reduced by 58% in the CCL2−/− DRG group, as compared with the CCL2+/+ DRG group, by day 4 of the co-culture assay (Fig. 4C–E, $p<0.05$, t-test). These results demonstrate that CCL2 expression by nerves facilitates both prostate cancer cell migration and perineural invasion.

CCR2 expression facilitates prostate cancer perineural in vivo

We next assessed the contribution of prostate cancer CCR2 expression in PNI using a murine *in vivo* model of sciatic nerve invasion. Sciatic nerve tumors generated from shControl PC-3 cells grew more rapidly than those generated from shCCR2 PC-3 cells, and shControl tumors at week 5 were of comparable volume to shCCR2 tumors at week 7 (Fig. 6A). To control for this growth differential, we compared perineural invasion between these groups at these two different time points, when overall tumor volume was equitable.

Functional assessment demonstrated that shControl tumors developed progressive, complete, ipsilateral hind limb paralysis over 5 weeks (Fig. 5B, 6B, 6C). In contrast, mice injected with shCCR2 PC-3 cells maintained intact sciatic nerve function over 5 weeks, with minimal additional functional deficits noted by 7 weeks (Fig. 5C, 6B, 6C). MRI imaging of shControl tumors showed anatomically thickened sciatic nerves at week 5 extending proximal to the primary tumors towards the spinal cord, consistent with PNI (Fig. 5E). In contrast, MRI imaging of shCCR2 tumors showed preservation of thin proximal sciatic nerves at week 7 (Fig. 5F), similar to those of normal mice lacking any tumor (Fig. 5A, 5D). Sciatic nerve invasion length was significantly greater for shControl tumors as compared with shCCR2 tumors ($p<0.05$, Sup. Fig. 5).

Clinical evaluation at the time of surgical exploration confirmed the MRI findings, demonstrating thickened and infiltrated proximal sciatic nerves for the shControl tumors at week 5 (Fig. 5H), as compared with normal appearing proximal sciatic nerves for the shCCR2 tumors at week 7 (Fig. 5I) and normal sciatic nerves in non-tumor bearing animals (Fig. 5G). Histological evaluation of excised sciatic nerves demonstrates extensive cancer infiltration in shControl tumors at week 5 (Fig. 7B), as compared to dramatically less cancer infiltration in shCCR2 tumors at week 7 (Fig. 7C), and normal nerves (Fig. 7A). Immunofluorescence microscopy demonstrated the presence of robust CCR2 expression in the shControl PC-3 tumors (Fig. 7D, E), but the absence of CCR2 expression in the shCCR2 PC-3 tumors (Fig. 7F, G), demonstrating that CCR2 silencing was sustained in shCCR2 PC-3 prostate tumors over the course of the animal experiments.

CCR2 is expressed in human prostate cancer specimens with perineural invasion

We assessed 24 human prostatectomy specimens, in which there were 34 distinct prostate adenocarcinomas that were spatially separated by normal prostatic tissue. These specimens were assessed with hematoxylin and eosin (H&E) staining and CCR2 immunohistochemistry (Fig. 8). Of the 34 distinct prostate cancers, there were 21 with histological evidence of PNI, and 13 without evidence of PNI. For the 21 cancers with PNI, 20 showed positive cytoplasmic expression of CCR2 (95%) by IHC. For the 13 cases without PNI, just 3 stained positive for CCR2 (23%). The distribution of CCR2 expression within the positive specimens was fairly uniform. Expression intensity was assessed to be 1+

for all of the positive specimens. Macrophage expression of CCR2 served as a positive control with 3+ expression intensity.

Discussion

Perineural invasion (PNI) is the process through which cancer cells invade and extend along nerves. PNI is an under-recognized and poorly understood route of metastatic spread (3). PNI in is a marker of poor prognosis for many malignancies, including pancreatic, prostate, head and neck, skin, salivary, colon, and other cancers (3, 30–32). Signaling between cancer cells and nerves through ligand-receptor interactions appears to be a key mechanism through which cancer cell migration towards and along nerves may be induced (3, 9, 12).

Chemokines are a family of small secreted molecules that play important roles in regulating immune cell recruitment during inflammatory responses and defense against foreign pathogens (33). Chemokines also may play roles in enabling cancer cell migration and metastases (15–17). Over 50 chemokines have been discovered and arranged into four different chemokine subfamilies, including the CC, CXC, XC, and CX3C subfamilies, depending on the number and spacing of the first two cysteine residues in the amino-terminal part of the protein (34). In addition to their roles in the immune system and in cancer progression, chemokines are also involved in nerve development, maintenance of nerve homeostasis, nerve injury repair, neuropathic pain and nerve inflammation (35). Because these varied roles may potentially intersect in PNI, we hypothesized that chemokine signaling may play a role in this process.

To identify novel chemokine ligands involved in PNI, we performed a chemokine screen of explants of murine DRG, which contain primarily neurons and glial cells. DRG explants in Matrigel sprout axonal-like projects which are analogous to tiny nerves, which in co-cultures with cancer cells serve as a model that recapitulates PNI (12, 27). Our screen identified CCL6 and CCL12, but these proteins have been identified only in rodents, and were therefore excluded from further consideration (36, 37). Chemerin, an adipokine regulating adipogenesis and adipocyte metabolism (38), was identified, as well as IL-16, which is expressed in bone marrow and spleen and acts as a T lymphocyte chemoattractant (39). However, the most plausible candidate identified on our chemokine screen to play a role in PNI was CCL2.

CCL2, also known as monocyte chemoattractant protein 1 (MCP-1), has demonstrated potent chemoattractic activity for monocytes, memory T cells, natural killer (NK) cells, and dendritic cells, resulting in the recruitment of these cells to sites of tissue injury and inflammation. CCL2 may activate both CCR2 and CCR4 receptors, although CCR2 is the predominant functional receptor for CCL2 (40, 41). CCL2-CCR2 signaling may activate p42/44 MAPK and PKC through G proteins to regulate cellular adhesion and motility in macrophages (42). In the nervous system, CCL2 is predominantly produced by microglial cells, astrocytes, and, to a lesser extent, by endothelial cells and neurons (43). In response to injury, CCL2 expression may be upregulated by various cell types of the nervous system, including Schwann cells, macrophages, endoneurial fibroblasts, and neurons. CCL2 may also play an important role in enhancing pain sensitivity and inducing chronic pain (44, 45).

Interestingly, CCR2 is expressed in a variety of cancer types and appears to play a role in cancer progression. Using immunohistochemical staining, 84% of prostate cancer samples express CCR2 (46). Higher CCR2 expression has also been associated with higher Gleason score and higher clinical pathologic stages (46). CCL2 may support prostate cancer survival and motility through binding to its receptor CCR2 (47). Similar effects of CCL2 have also been found in breast cancer and hepatoma cells (48, 49).

We reasoned that the varied roles of CCL2 function as a (a) chemoattractant, (b) factor released with neural injury, and (c) factor promoting cancer progression, might all plausibly intersect in the process of perineural invasion. Cancer infiltration into nerves might induce a form of nerve injury that releases CCL2, which may then induce a nerve repair inflammatory response, induce the migration of CCR2 expressing cancer cells towards these nerves, and ultimately promote PNI.

We demonstrate here that CCR2-expressing prostate cancer cells are able to migrate towards CCL2 and DRG. In contrast, cells lacking CCR2 fail to migrate towards CCL2, and migration towards DRG is diminished, but not abrogated, suggesting that other nerve secreted factors additionally support cancer cell migration. Using an *in vitro* co-culture assay of PNI with DRG harvested from CCL2 −/− mice, we demonstrate that both (a) CCL2 release by the DRG and (b) CCR2 expression by the prostate cancer cells significantly enable PNI. Using an *in vivo* murine sciatic nerve model of PNI, prostate cancer cells lacking CCR2 show a dramatically reduced ability to invade nerves and impair nerve function. Finally, human prostate cancer specimens demonstrated a very high rate of CCR2 expression (95%) in tumors with PNI, but a considerably lower rate of CCR2 expression in tumors lacking PNI (23%). This correlation between the rate of CCR2 expression and the presence of PNI in human clinical specimens further supports the concept that CCR2 is likely playing a mechanistic role in the process of PNI.

Clearly, other neurotrophic factors may be additionally contributing to the mechanisms underlying PNI. When live explants of DRG in Matrigel are used to attract PC-3, more robust migration is demonstrated than with CCL2 alone (Fig. 2E), suggesting the presence of other nerve secreted factors facilitating migration. Our group previously demonstrated the role that GDNF-RET signaling plays in pancreatic cancer PNI, and others groups have explored the contributions of other nerve-released ligands including NGF, artemin, CX3CL1, BDNF, and others (9). It is possible that a spectrum of these molecules may be at play in supporting the process of PNI, varying to some degree with each cancer's particular molecular profile of cell surface receptors dictating a chemotactic response to each nerve secreted ligand. Other nerve-released factors may also potentiate PNI by having effects on cancer cell adhesion, motility, and proliferation. The recent development of CCR2 antagonists raises the possibility that CCL2-CCR2 signaling may be pharmacologically targeted (50). Therapeutically blocking the molecular mechanism underlying a cancer's particular adverse phenotype, rather than simply targeting cell viability, represents an innovative approach towards cancer management that merits further study.

In conclusion, we identify CCL2-CCR2 signaling as playing a significant role in PNI by prostate cancer. PNI holds clinical significance as an adverse prognostic factor for a variety

of malignancies; however, its underlying mechanisms remain complex and poorly understood. Communication between cancer cells and the nerve microenvironment may occur through a variety of mechanisms, and CCL2-CCR2 signaling appears to play a fundamental role. These results reveal a novel molecular target in PNI for potential future therapeutic intervention.

Supplementary Material

Refer to Web version on PubMed Central for supplementary material.

Acknowledgments

We thank Ke Xu and Tatiana A. Omelchenko for assistance with microscopic imaging. SZH is grateful to Dr. Demin Han and Dr. Jatin P. Shah for supporting his fellowship.

RJW is supported by R01CA157686. SZH and ZKY were supported by the Beijing Municipal Health Bureau Grant 2009208. SBH was supported by Anhui Provincial Natural Science Foundation 1308085MH131.

References

1. Siegel R, Naishadham D, Jemal A. Cancer statistics, 2012. CA: a cancer journal for clinicians. 2012; 62:10–29. [PubMed: 22237781]
2. Harnden P, Shelley MD, Clements H, Coles B, Tyndale-Biscoe RS, Naylor B, et al. The prognostic significance of perineural invasion in prostatic cancer biopsies: a systematic review. Cancer. 2007; 109:13–24. [PubMed: 17123267]
3. Liebig C, Ayala G, Wilks JA, Berger DH, Albo D. Perineural invasion in cancer: a review of the literature. Cancer. 2009; 115:3379–91. [PubMed: 19484787]
4. Fromont G, Godet J, Pires C, Yacoub M, Dore B, Irani J. Biological significance of perineural invasion (PNI) in prostate cancer. The Prostate. 2012; 72:542–8. [PubMed: 21748758]
5. Maru N, Ohori M, Kattan MW, Scardino PT, Wheeler TM. Prognostic significance of the diameter of perineural invasion in radical prostatectomy specimens. Human pathology. 2001; 32:828–33. [PubMed: 11521227]
6. Ayala GE, Dai H, Ittmann M, Li R, Powell M, Frolov A, et al. Growth and survival mechanisms associated with perineural invasion in prostate cancer. Cancer research. 2004; 64:6082–90. [PubMed: 15342391]
7. DeLancey JO, Wood DP Jr, He C, Montgomery JS, Weizer AZ, Miller DC, et al. Evidence of perineural invasion on prostate biopsy specimen and survival after radical prostatectomy. Urology. 2013; 81:354–7. [PubMed: 23374801]
8. Hassan MO, Maksem J. The prostatic perineural space and its relation to tumor spread: an ultrastructural study. The American journal of surgical pathology. 1980; 4:143–8. [PubMed: 6155085]
9. Bapat AA, Hostetter G, Von Hoff DD, Han H. Perineural invasion and associated pain in pancreatic cancer. Nature reviews Cancer. 2011; 11:695–707.
10. Binmadi NO, Basile JR. Perineural invasion in oral squamous cell carcinoma: a discussion of significance and review of the literature. Oral oncology. 2011; 47:1005–10. [PubMed: 21865078]
11. Marchesi F, Piemonti L, Mantovani A, Allavena P. Molecular mechanisms of perineural invasion, a forgotten pathway of dissemination and metastasis. Cytokine & growth factor reviews. 2010; 21:77–82. [PubMed: 20060768]
12. Gil Z, Cavel O, Kelly K, Brader P, Rein A, Gao SP, et al. Paracrine regulation of pancreatic cancer cell invasion by peripheral nerves. Journal of the National Cancer Institute. 2010; 102:107–18. [PubMed: 20068194]

13. Bakst RL, Lee N, He S, Chernichenko N, Chen CH, Linkov G, et al. Radiation impairs perineural invasion by modulating the nerve microenvironment. PloS one. 2012; 7:e39925. [PubMed: 22768171]
14. Fernandez EJ, Lolis E. Structure, function, and inhibition of chemokines. Annual review of pharmacology and toxicology. 2002; 42:469–99.
15. Balkwill F. Cancer and the chemokine network. Nature reviews Cancer. 2004; 4:540–50.
16. Murphy PM. Chemokines and the molecular basis of cancer metastasis. The New England journal of medicine. 2001; 345:833–5. [PubMed: 11556308]
17. Kulbe H, Levinson NR, Balkwill F, Wilson JL. The chemokine network in cancer--much more than directing cell movement. The International journal of developmental biology. 2004; 48:489–96. [PubMed: 15349823]
18. Roussos ET, Condeelis JS, Patsialou A. Chemotaxis in cancer. Nature reviews Cancer. 2011; 11:573–87.
19. Muller A, Homey B, Soto H, Ge N, Catron D, Buchanan ME, et al. Involvement of chemokine receptors in breast cancer metastasis. Nature. 2001; 410:50–6. [PubMed: 11242036]
20. Kakinuma T, Hwang ST. Chemokines, chemokine receptors, and cancer metastasis. Journal of leukocyte biology. 2006; 79:639–51. [PubMed: 16478915]
21. Ben-Baruch A. Organ selectivity in metastasis: regulation by chemokines and their receptors. Clinical & experimental metastasis. 2008; 25:345–56. [PubMed: 17891505]
22. Taichman RS, Cooper C, Keller ET, Pienta KJ, Taichman NS, McCauley LK. Use of the stromal cell-derived factor-1/CXCR4 pathway in prostate cancer metastasis to bone. Cancer research. 2002; 62:1832–7. [PubMed: 11912162]
23. Uehara H, Troncoso P, Johnston D, Bucana CD, Dinney C, Dong Z, et al. Expression of interleukin-8 gene in radical prostatectomy specimens is associated with advanced pathologic stage. The Prostate. 2005; 64:40–9. [PubMed: 15651067]
24. van Golen KL, Ying C, Sequeira L, Dubyk CW, Reisenberger T, Chinnaiyan AM, et al. CCL2 induces prostate cancer transendothelial cell migration via activation of the small GTPase Rac. Journal of cellular biochemistry. 2008; 104:1587–97. [PubMed: 18646053]
25. Jia T, Leiner I, Dorothee G, Brandl K, Pamer EG. MyD88 and Type I interferon receptor-mediated chemokine induction and monocyte recruitment during Listeria monocytogenes infection. Journal of immunology (Baltimore, Md : 1950). 2009; 183:1271–8.
26. Tonge DA, Golding JP, Edbladh M, Kroon M, Ekstrom PE, Edstrom A. Effects of extracellular matrix components on axonal outgrowth from peripheral nerves of adult animals in vitro. Experimental neurology. 1997; 146:81–90. [PubMed: 9225741]
27. Ayala GE, Wheeler TM, Shine HD, Schmelz M, Frolov A, Chakraborty S, et al. In vitro dorsal root ganglia and human prostate cell line interaction: redefining perineural invasion in prostate cancer. The Prostate. 2001; 49:213–23. [PubMed: 11746267]
28. Hu D, Hu R, Berde CB. Neurologic evaluation of infant and adult rats before and after sciatic nerve blockade. Anesthesiology. 1997; 86:957–65. [PubMed: 9105240]
29. Roca H, Varsos Z, Pienta KJ. CCL2 protects prostate cancer PC3 cells from autophagic death via phosphatidylinositol 3-kinase/AKT-dependent survivin up-regulation. The Journal of biological chemistry. 2008; 283:25057–73. [PubMed: 18611860]
30. Pour PM, Bell RH, Batra SK. Neural invasion in the staging of pancreatic cancer. Pancreas. 2003; 26:322–5. [PubMed: 12717262]
31. Feng FY, Qian Y, Stenmark MH, Halverson S, Blas K, Vance S, et al. Perineural invasion predicts increased recurrence, metastasis, and death from prostate cancer following treatment with dose-escalated radiation therapy. International journal of radiation oncology, biology, physics. 2011; 81:e361–7.
32. Johnston M, Yu E, Kim J. Perineural invasion and spread in head and neck cancer. Expert review of anticancer therapy. 2012; 12:359–71. [PubMed: 22369327]
33. Mackay CR. Chemokines: immunology's high impact factors. Nature immunology. 2001; 2:95–101. [PubMed: 11175800]
34. Charo IF, Ransohoff RM. The many roles of chemokines and chemokine receptors in inflammation. The New England journal of medicine. 2006; 354:610–21. [PubMed: 16467548]

35. White FA, Jung H, Miller RJ. Chemokines and the pathophysiology of neuropathic pain. Proceedings of the National Academy of Sciences of the United States of America. 2007; 104:20151–8. [PubMed: 18083844]

36. Kanno M, Suzuki S, Fujiwara T, Yokoyama A, Sakamoto A, Takahashi H, et al. Functional expression of CCL6 by rat microglia: a possible role of CCL6 in cell-cell communication. Journal of neuroimmunology. 2005; 167:72–80. [PubMed: 16087246]

37. Moore BB, Murray L, Das A, Wilke CA, Herrygers AB, Toews GB. The role of CCL12 in the recruitment of fibrocytes and lung fibrosis. American journal of respiratory cell and molecular biology. 2006; 35:175–81. [PubMed: 16543609]

38. Bondue B, Wittamer V, Parmentier M. Chemerin and its receptors in leukocyte trafficking, inflammation and metabolism. Cytokine & growth factor reviews. 2011; 22:331–8. [PubMed: 22119008]

39. Wilson KC, Center DM, Cruikshank WW. The effect of interleukin-16 and its precursor on T lymphocyte activation and growth. Growth factors (Chur, Switzerland). 2004; 22:97–104.

40. Jung H, Bhangoo S, Banisadr G, Freitag C, Ren D, White FA, et al. Visualization of chemokine receptor activation in transgenic mice reveals peripheral activation of CCR2 receptors in states of neuropathic pain. The Journal of neuroscience : the official journal of the Society for Neuroscience. 2009; 29:8051–62. [PubMed: 19553445]

41. Fife BT, Huffnagle GB, Kuziel WA, Karpus WJ. CC chemokine receptor 2 is critical for induction of experimental autoimmune encephalomyelitis. The Journal of experimental medicine. 2000; 192:899–905. [PubMed: 10993920]

42. Jimenez-Sainz MC, Fast B, Mayor F Jr, Aragay AM. Signaling pathways for monocyte chemoattractant protein 1-mediated extracellular signal-regulated kinase activation. Molecular pharmacology. 2003; 64:773–82. [PubMed: 12920215]

43. Harkness KA, Sussman JD, Davies-Jones GA, Greenwood J, Woodroofe MN. Cytokine regulation of MCP-1 expression in brain and retinal microvascular endothelial cells. Journal of neuroimmunology. 2003; 142:1–9. [PubMed: 14512159]

44. White FA, Feldman P, Miller RJ. Chemokine signaling and the management of neuropathic pain. Molecular interventions. 2009; 9:188–95. [PubMed: 19720751]

45. Van Steenwinckel J, Reaux-Le Goazigo A, Pommier B, Mauborgne A, Dansereau MA, Kitabgi P, et al. CCL2 released from neuronal synaptic vesicles in the spinal cord is a major mediator of local inflammation and pain after peripheral nerve injury. The Journal of neuroscience : the official journal of the Society for Neuroscience. 2011; 31:5865–75. [PubMed: 21490228]

46. Lu Y, Cai Z, Xiao G, Liu Y, Keller ET, Yao Z, et al. CCR2 expression correlates with prostate cancer progression. Journal of cellular biochemistry. 2007; 101:676–85. [PubMed: 17216598]

47. Lu Y, Chen Q, Corey E, Xie W, Fan J, Mizokami A, et al. Activation of MCP-1/CCR2 axis promotes prostate cancer growth in bone. Clinical & experimental metastasis. 2009; 26:161–9. [PubMed: 19002595]

48. Fang WB, Jokar I, Zou A, Lambert D, Dendukuri P, Cheng N. CCL2/CCR2 chemokine signaling coordinates survival and motility of breast cancer cells through Smad3 protein- and p42/44 mitogen-activated protein kinase (MAPK)-dependent mechanisms. The Journal of biological chemistry. 2012; 287:36593–608. [PubMed: 22927430]

49. Dagouassat M, Suffee N, Hlawaty H, Haddad O, Charni F, Laguillier C, et al. Monocyte chemoattractant protein-1 (MCP-1)/CCL2 secreted by hepatic myofibroblasts promotes migration and invasion of human hepatoma cells. International journal of cancer. Journal international du cancer. 2010; 126:1095–108. [PubMed: 19642141]

50. Xue CB, Wang A, Meloni D, Zhang K, Kong L, Feng H, et al. Discovery of INCB3344, a potent, selective and orally bioavailable antagonist of human and murine CCR2. Bioorg med chem lett. 2010; 20:7473–8. [PubMed: 21036044]

Implications

These results reveal CCL2-CCR2 signaling as a key ligand-receptor mechanism that mediates cancer cell communication with nerves during PNI and highlight a potential future therapeutic target.

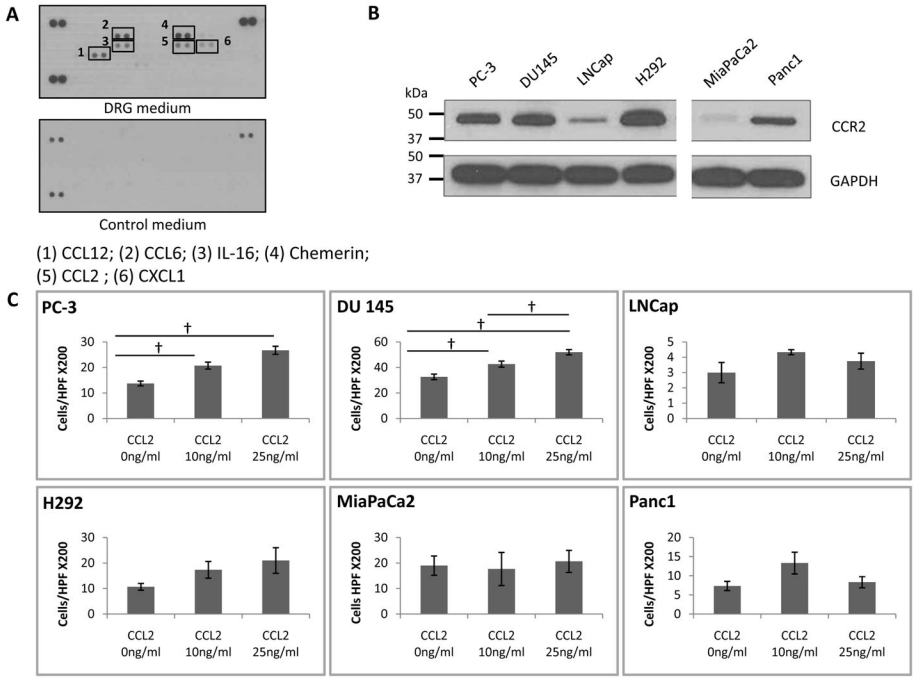

Fig. 1. CCL2 is expressed by dorsal root ganglia (DRG), and induces migration by CCR2-expressing cancer cells

A. Chemokine array of DRG conditioned medium, with DMEM media as a control, identifies the expression of CCL2, CCL6, CCL12, IL-16 and chemerin. B. The expression of CCR2 (42kD) is variable in a panel of six cancer cell lines, including prostate (PC-3, DU145, LNCap), salivary mucoepidermoid (H292), and pancreatic (MiPaCa-2 and Panc1) by Western blot. C. Boyden chamber migration assays of the six cancer cell lines, using CCL2 as an attractant, shows that the migratory response to CCL2 generally correlates with CCR2 expression († $p<0.05$, N=3 experiments).

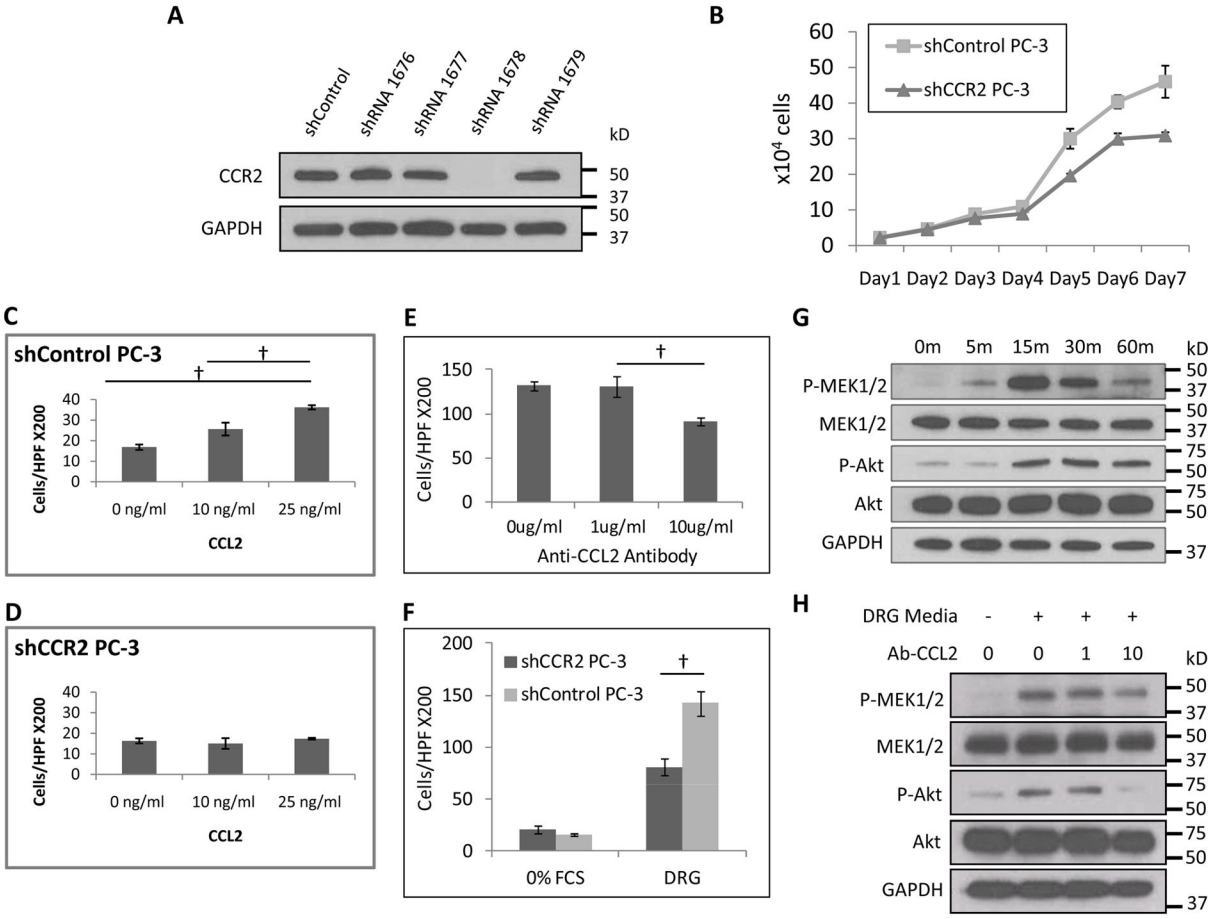

Fig. 2. CCR2 is required for CCL2 induced cancer migration, and CCL2 released by DRG induces cancer migration

A. Expression of CCR2 was measured in PC-3 cells after undergoing transfection with a panel of shRNAs targeting CCR2, or control shRNA. The 1678 short hairpin was used to create stably silenced shCCR2 PC-3 cells. B. Cell proliferation of shControl and shCCR2 PC-3 cells is similar through 4 days, followed by a mildly increased rate by the shControl cells. C. Boyden chamber migration assays over 18 hours were performed using CCL2 as an attractant for shControl PC-3 cells, which show dose-response migration. († $p<0.05$, t-test, N=3). D. Migration assays were performed using CCL2 as an attractant for shCCR2 PC-3 cells, which show a lack of migratory response. E. Migration assays were performed using conditioned media from DRG as an attractant for PC-3 cells. A blocking anti-CCL2 antibody was added at varying concentrations to assess the relative contributions of CCL2 signaling in DRG-induced PC-3 migration († $p<0.05$, t-test, N=3). F. Migration assays were performed using conditioned media or media with 0% FCS as an attractant for shControl and shCCR2 PC-3 cells († $p<0.05$, t-test, N=3). G. PC-3 cells were exposed to 25ng/ml CCL2, and protein isolated at varying times for Western blotting to assess p-MEK1/2 and p-Akt activity. H. PC-3 cells were exposed to conditioned media from DRG, and treated with varying concentrations of anti-CCL2 antibody to assess effects on p-MEK1/2 and p-Akt activity.

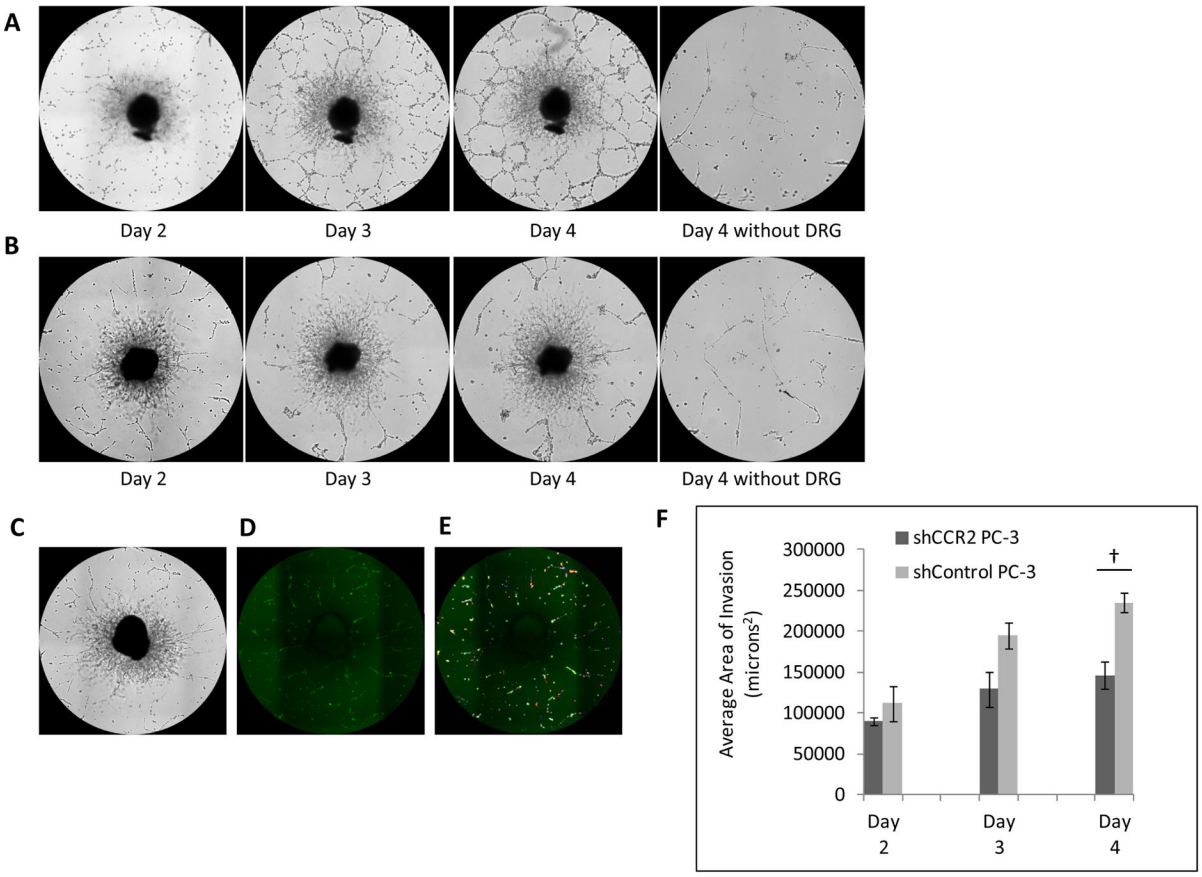

Fig. 3. CCR2 expression by prostate cancer facilitates perineural invasion in vitro

Dorsal root ganglia (DRG) and cancer co-culture assay of PNI permits the assessment of interactions between cancer and nerve cells. A. shControl PC-3 cells exhibit progressive cancer cell invasion along DRG neurites from days 2 to 4. B. In contrast, shCCR2 PC-3 cells demonstrate diminished invasion along DRG neurites from days 2 to 4. Cancer cells fail to significantly invade the Matrigel drop in the absence of a DRG. C–E. A method was developed to quantify the degree of PNI in DRG-cancer co-culture assays (C). Green fluorescent PC-3 cells (D) invading the DRG are measured by MetaMorph software (E) and the area of invading cells is quantified. F. The average area of perineural invasion was quantified and compared between shControl and shCCR2 PC-3 groups from days 2 to 4 († $p<0.05$, t-test, N=3).

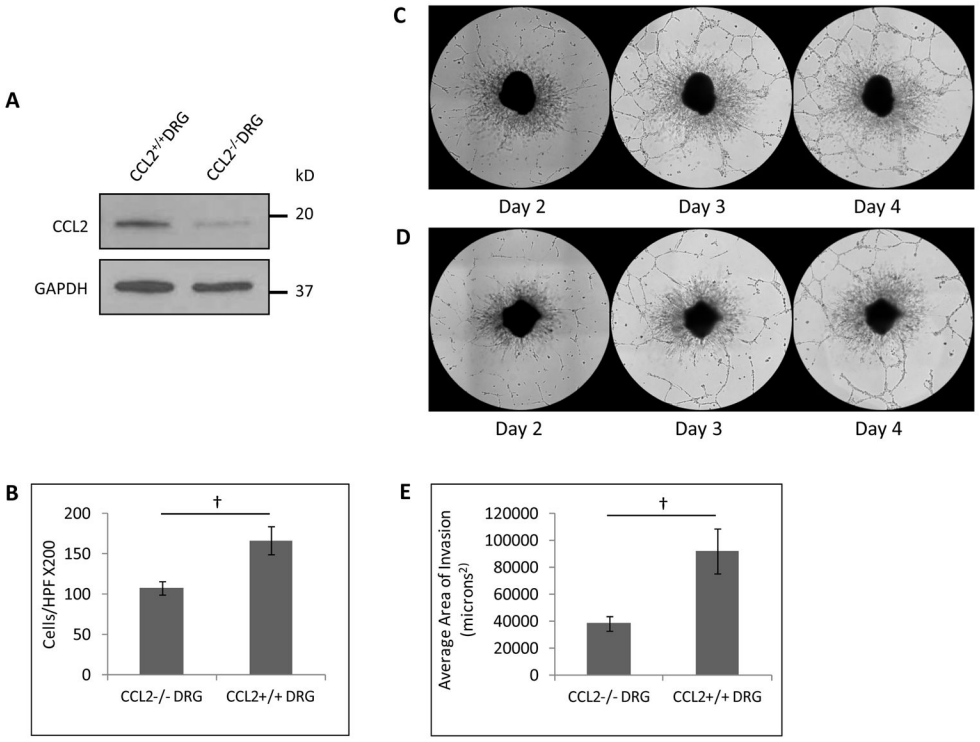

Fig. 4. CCL2 release by DRG facilitates prostate cancer migration and perineural invasion in vitro

A. Western blot demonstrates a reduction of CCL2 expression by DRG harvested from CCL2−/− mice as compared with CCL2+/+ mice. B. Boyden chamber assay demonstrates differential migration of PC-3 cells towards CCL2−/− DRG as compared to CCL2+/+ DRG († $p<0.05$, t-test). C. DRG-cancer co-culture assays of PC-3 cells with CCL2+/+ DRG demonstrate association of cancer cells with neurites from days 2 to 4. D. In contrast, DRG-cancer co-culture assays of PC-3 cells with CCL2−/− DRG demonstrate a reduction of cancer cell association with neurites. E. The average area of perineural invasion was quantified and compared between the CCL2−/− DRG and CCL2+/+ DRG at day 4 († $p<0.05$, t-test).

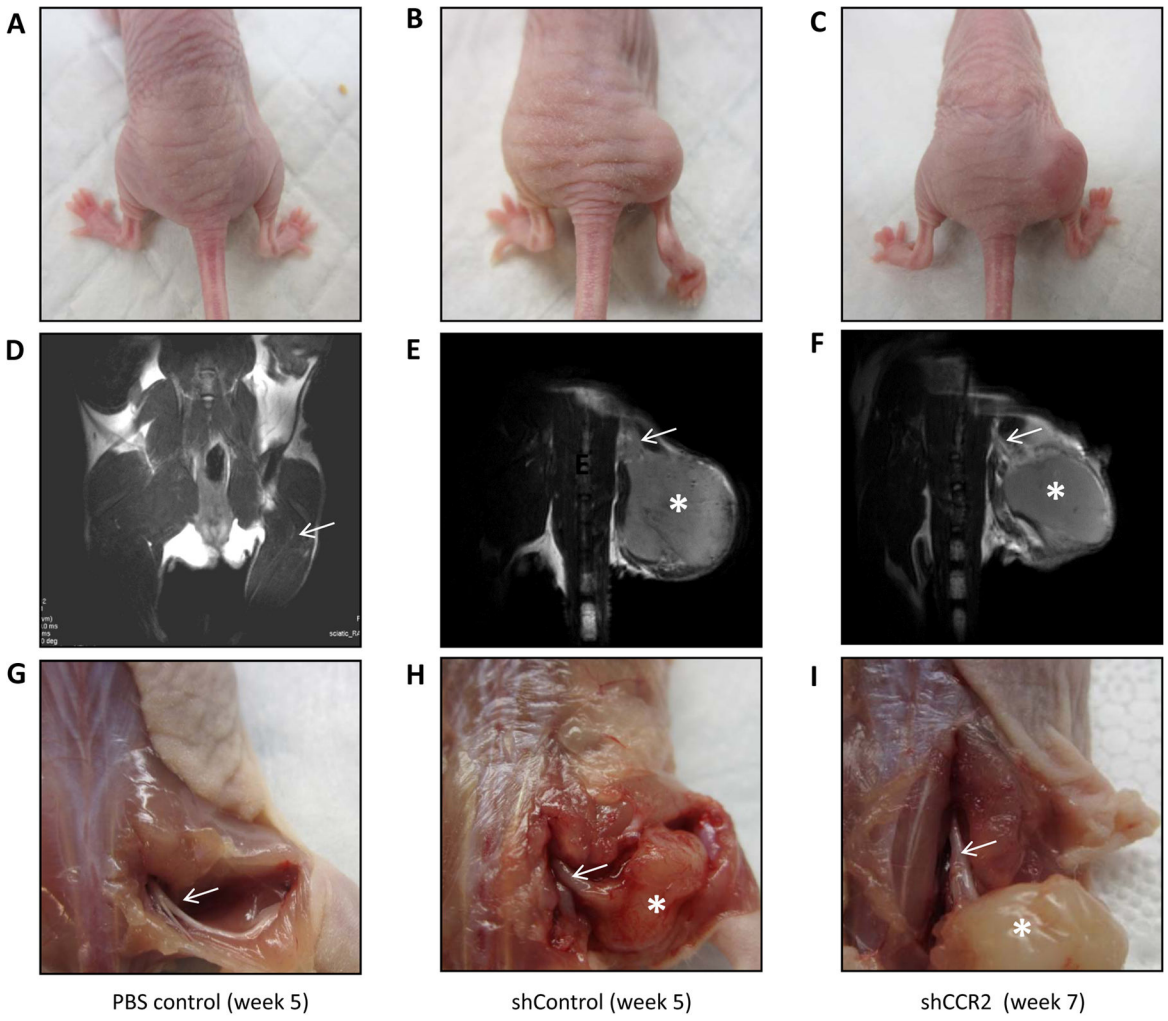

Fig. 5. CCR2 expression facilitates prostate cancer perineural in vivo by magnetic resonance imaging

A–C. A murine sciatic nerve model was used to assess PNI, and representative photos are demonstrated for each group. A mouse injected with PBS into the right sciatic nerve demonstrates normal right hind limb position (A) at week 5 after injection. A mouse injected with shControl PC-3 into the right sciatic nerve demonstrates paralysis of the right hind limb 5 weeks after injection (B), while a mouse injected with shCCR2 PC-3 into the right sciatic nerve maintains intact right hind limb motion 7 weeks after injection (C). D–F. MRI T2 weighted images were taken of mice under anesthesia to visualize the proximal sciatic nerve to assess for PNI. A mouse injected with PBS into the right sciatic nerve shows a thin, normal sciatic nerve at week 5 after injection (D). The MRI image of a mouse injected with shControl PC-3 shows a thickened sciatic nerve (arrow) coursing proximal to the injected tumor mass in the sciatic nerve (asterisk) at week 5 after injection (E). In contrast, the right sciatic nerve of a mouse injected with shCCR2 PC-3 demonstrates tumor at the sciatc nerve injection local site (asterisk), but a nearly normal proximal sciatic nerve caliber (arrow) at week 7 after injection (F). At the time of animal sacrifice, sciatic nerve tumors and the proximal sciatic were surgically exposed. A PBS injected sciatic nerve appears thin and

shiny at week 5 after injection (G). A shControl PC-3 sciatic nerve tumor (asterisk) shows evidence of proximal sciatic nerve invasion and thickening (arrow) consistent with PNI (H). A shCCR2 PC-3 sciatic nerve tumor (asterisk) demonstrates a short distance of nerve thickening, which rapidly tapers to a normal caliber nerve, showing a lesser degree of PNI (I). Comparisons were performed at times of similar tumor volume between the shControl and shCCR2 tumor groups.

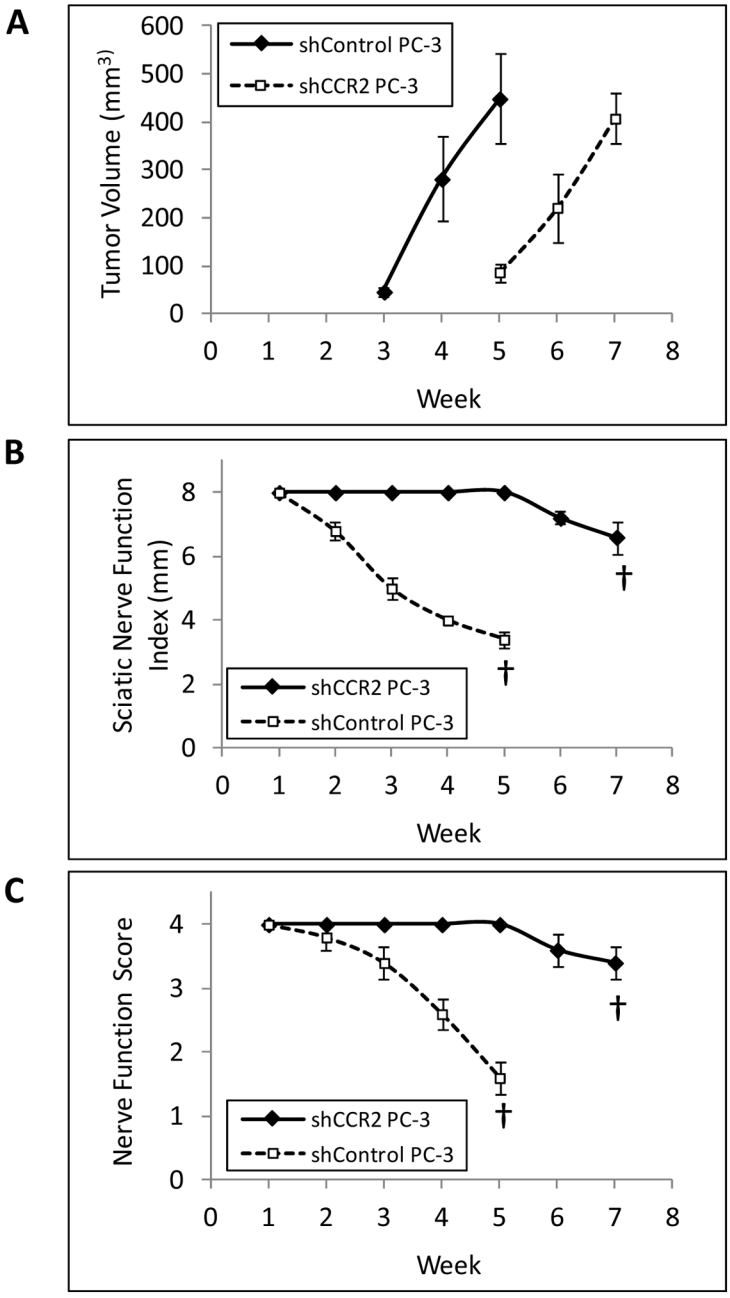

Fig. 6. CCR2 expression enhances neurologic functional deficits resulting from perineural invasion

A. The shControl PC-3 sciatic nerve tumors grew more rapidly *in vivo* as compared with the shCCR2 PC-3 tumors (n=5 per group). We noted that tumors volumes were equitable at week 5 for shControl, as compared with week 7 for shCCR2. We performed comparisons of neurologic function at these two different time points, to control for tumor volume as a potential confounding variable. B. The sciatic nerve index (hind paw span width) demonstrated significant differences between shControl at week 5 with shCCR2 at week 7 († $p<0.001$, t-test). C. The mean sciatic nerve function score is determined by hind limb

function (ranging from normal to complete paralysis) and demonstrated significant differences between shControl at week 5 with shCCR2 at week 7 († $p<0.001$, t-test).

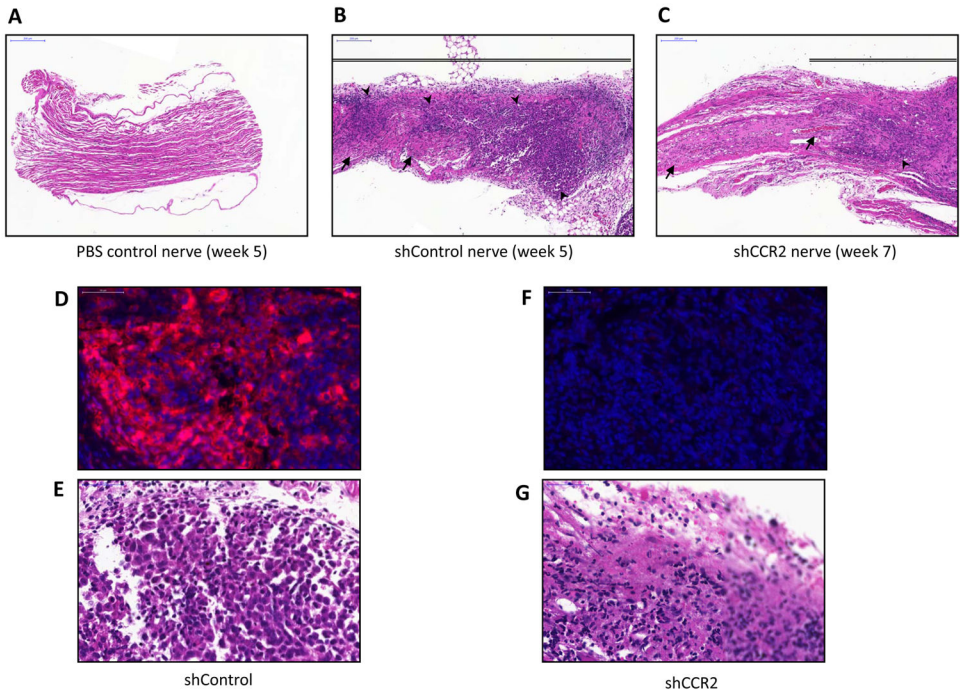

Fig. 7. CCR2 expression facilitates prostate cancer perineural invasion in vivo by histology

Histology was performed of representative excised murine sciatic nerves from each group. A. Hematoxylin and eosin (H&E) staining of a PBS control sciatic nerve demonstrates normal nerve histology (bar, 200μm). B. H&E staining of shControl PC-3 sciatic nerves 5 weeks after injection demonstrate extensive cancer invasion and infiltration within the thickened nerve (bar, 200μm). C. H&E staining of shCCR2 PC-3 sciatic nerves sciatic nerves 7 weeks after injection demonstrate a reduced degree of cancer invasion of the nerve (bar, 200μm). D. Immunofluorescence (IF) microscopy for CCR2 (red) with DAPI nuclear staining (blue) shows intact CCR2 expression by shControl PC-3 tumors 5 weeks after injection (bar, 50 μm). E. H&E stained shControl PC-3 tumors are shown 5 weeks after injection. F. IF microscopy shows a lack of CCR2 expression in the shCCR2 PC-3 tumors 7 weeks after injection (bar, 50 μm). G. H&N stained shCCR2 PC-3 tumors are shown 7 weeks after injection.

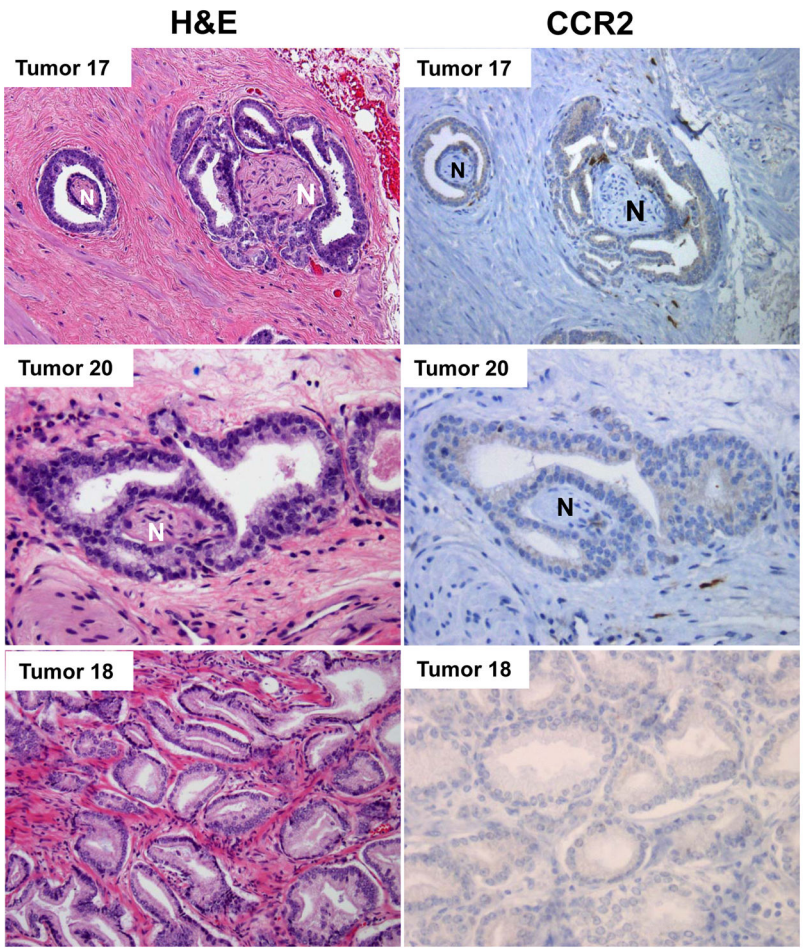

Fig. 8. CCR2 is expressed in human prostate cancer specimens with perineural invasion

Tumors 17 and 20 are human prostate adenocarcinomas with PNI, which demonstrate positive staining of CCR2 by immunohistochemistry (N – nerve, H&E – hematoxylin and eosin). In contrast, Tumor 18 is a human prostate adenocarcinoma without PNI that fails to express CCR2. Of 21 prostate adenocarcinomas with histological evidence of PNI, 20 showed positive cytoplasmic expression of CCR2 (95%) by immunohistochemistry (IHC). In contrast, out of 13 cases without PNI, just 3 stained positive for CCR2 (23%).